Linear stability analysis of force-free equilibria close to Taylor relaxed states

E. Tassi[a)]
CNISM and Burning Plasma Research Group, Dipartimento di Energetica, Politecnico di Torino, Corso Duca degli Abruzzi 24, 10129 Torino, Italy

R. J. Hastie
Burning Plasma Research Group, Dipartimento di Energetica, Politecnico di Torino, Corso Duca degli Abruzzi 24, 10129 Torino, Italy and Culham Science Centre, EURATOM/UKAEA Fusion Association, Abingdon, OX14 3DB, United Kingdom

F. Porcelli
Burning Plasma Research Group, Dipartimento di Energetica, Politecnico di Torino, Corso Duca degli Abruzzi 24, 10129 Torino, Italy

(Received 9 March 2007; accepted 16 July 2007; published online 20 September 2007)

The linear stability of a class of force-free equilibria in cylindrical geometry is investigated. The class consists of cylindrically symmetric force-free equilibria for which the ratio μ between the parallel current density and the magnetic field is a step function of the radius. It is suggested that plasmas in reversed field pinches could be roughly represented by such equilibria as a consequence of a small departure from an initial force-free state with constant μ, the latter being reached after a relaxation process according to the classical theory proposed by Taylor [Phys. Rev. Lett. **33**, 1139 (1974)]. A fully analytical derivation of the tearing stability parameter Δ' for such class of equilibria is given. It is then shown with one explicit example how the presence of a downward step of relatively small height can destabilize the innermost resonant mode, which would otherwise be stable if μ were constant. A possible implication of this mechanism for the formation of cyclic quasisingle helicity states observed in reversed field pinches is proposed. Considerations on the ideal stability of the class of equilibria under investigation are also given. © *2007 American Institute of Physics*. [DOI: 10.1063/1.2769324]

I. INTRODUCTION

Plasmas confined in reverse field pinch (RFP) experiments have been studied now for nearly five decades.[1] Earliest observations[2] recorded a transition from a highly turbulent state to a less turbulent one, originally described as the quiescent state, accompanied by a spontaneous and surprising reversal of the toroidal magnetic field at the plasma edge. A theoretical interpretation for this phenomenon of spontaneous field reversal was provided by Taylor in a series of papers[3] describing the process in terms of a relaxation phenomenon under certain global constraints, namely, conservation of toroidal flux Φ and of helicity $K=\int \mathbf{A}\cdot\mathbf{B}d^3x$, where $\mathbf{B}=\nabla\times\mathbf{A}$ is the magnetic field and $\mathbf{A}$ is the vector potential. According to this theory, the mean plasma current density in the relaxed state is parallel to the mean magnetic field, $\mathbf{J}=\mu\mathbf{B}$, with μ=constant. The evolution towards a relaxed state is thought to be caused by the nonlinear evolution of reconnecting magnetohydrodynamic (MHD) modes, involving several poloidal, m, and toroidal, n, mode numbers. Therefore, according to Taylor's theory, the relaxed state might be viewed as the superposition of a mean, force-free field, where $\mathbf{J}$ is parallel to $\mathbf{B}$, superimposed on a broad spectrum of low amplitude magnetic turbulence. In particular if the value of the global helicity $\hat{K}$ (see below in Sec. II) is less than a critical value, then the mean field is cylindrically symmetric, otherwise helically symmetric states are the preferred states for they possess lower magnetic energy. This situation is often proposed as the natural description of standard RFP operation. The plasma state in this standard condition is usually termed *multiple-helicity*, or MH-state, where "multiple helicity" refers to the presence of MHD fluctuations involving several helicities, i.e., several values of m/n.

Taylor's relaxed state should not be considered as a steady state equilibrium in a strict sense, but as a *quasiequilibrium* on time scales that are short on the resistive evolution time. Indeed, as a consequence of plasma heating and resistive diffusion, the mean current density tends to evolve away from the relaxed state. This resistive evolution may still maintain the mean $\mathbf{J}$ nearly parallel to the mean $\mathbf{B}$, at least initially, but with a nonconstant μ-profile, e.g., $\mu=\mu(r)$. We also point out that the relaxed state with $\mathbf{J}\times\mathbf{B}=\mathbf{0}$ and μ=constant is necessarily an idealized state, as it presumes force balance with a flat pressure profile and does not take into account realistic boundary conditions at the conducting plasma wall, where the current density should vanish.

Recognizing that resistive evolution indeed tends to produce nonconstant μ profiles, as well as nonconstant pressure profiles, one may notice that these profiles could become unstable[1] to tearing modes[4] that are resonant on magnetic surfaces where the magnetic winding index $q(r)=m/n$. Fur-

a)Electronic mail: emanuele.tassi@polito.it

thermore, in RFP devices the average field-line curvature is unfavorable, so that pressure driven g-modes of tearing parity are easily excited[5] and will generate small magnetic islands, even in the presence of large negative values of the tearing stability index,[6] Δ'. If these unstable modes involved several values of m/n, they could represent the very cause of plasma relaxation to Taylor's state. The ideal and resistive stability of force-free equilibria with a nonconstant μ-profile was also considered in Refs. 7–9.

However, an apparent departure from Taylor's theory relates to recent experimental observations of plasma states with a near-helical symmetry, i.e., states where the Fourier decomposition of the magnetic field is dominated by components with a well defined value of m/n, in addition to the dominant $m=0$, $n=0$ component of MH-states. These so-called quasisingle helicity (QSH) states have been discovered on various RFP experiments.[10–15] The QSH states are very interesting, in that it has been conjectured[14] that they could lead to improved confinement conditions as compared with the MH-states. Indeed, an improvement in particle confinement has been reported in Ref. 16.

Typically, the value m/n of the dominant helicity observed experimentally corresponds to $m=1$ and n such that the corresponding perturbation is resonant closest to the magnetic axis, i.e., $n=\text{integer}[1+q_0^{-1}]$. We shall refer to this as the *central resonance*. The QSH states at first sight appear to be inconsistent with Taylor's theory. We point out that Taylor's theory predicts the existence of relaxed states with helical symmetry. These states require a value of $\hat{\mu}=\mu a$, where a is the cylinder radius, corresponding to the critical value, $\hat{\mu}_{\text{crit}}=3.11$ (for simplicity hats are dropped in the remainder of the paper and so μ indicates a dimensionless quantity). However, Taylor's helical states possess a chirality (i.e., a sign of m/n) that is opposite to the one observed experimentally, as they are associated with a mode that is resonant near the plasma edge, where q is negative.

An important research line[14,17–19] assumes that the QSH states are equilibria in a strict sense, i.e., are solutions of the equilibrium helical Grad-Shafranov equation subject to the Ohmic constraint. This explanation of the QSH states would lead to a new picture of RFPs, far from Taylor's original idea. While numerical investigations seem to support this new picture, a fully satisfactory analytic understanding of the QSH states as force free helical equilibria consistent with Ohm's law is still elusive. We point out that in experiments the observed helical structures are intermittent in time and limited to relatively small volumes.[20] The picture emerging from recent RFX (Reversed Field eXperiment) experiments (see, e.g., Fig. 11 in Ref. 20) is that the plasma settles in QSH states for relatively short periods of time, as compared with the resistive evolution time scale. During one such period, a dominant $m=1$ tearing mode, with an n-value corresponding to the central resonance (e.g., $n=7$ in Ref. 20), grows steadily to relatively large amplitude, at which point a rapid relaxation event appears to terminate this phase, before the cycle repeats. The dominant tearing mode appears, therefore, to play a similar role to that of the $m/n=1/1$ precursor oscillation in the tokamak sawtooth phenomenon.[21] However, unlike sawtooth relaxation events in tokamaks, the single helicity (1,7) precursor is accompanied throughout by a lower level of many other $m=1$ modes. Those with $n=8,9,10\ldots$ correspond to tearing modes with resonant surface locations between that of the $n=7$ and the reversal radius where $B_z=0$. One possible explanation of the difference between tokamak and RFP behavior lies in the differing role of pressure driven modes in the two devices. As we pointed out earlier in this discussion, the average magnetic curvature in a RFP is unfavorable, while in a tokamak it is such as to inhibit pressure driven modes in the plasma region where q is above unity. The recent observation of cyclic QSH behavior in RFX has been facilitated by the inclusion of feedback coils, which have been very successful in prolonging the discharge duration to over six wall times by essentially eliminating the damaging plasma-wall interactions generated by resistive wall modes.[20]

In this paper, we seek to explain the QSH state as a small, cyclic departure from a Taylor state, rather than as a radically different equilibrium scenario. The reference Taylor state we consider is characterized by a value of $\mu=\mu_T=\text{constant}$ in the range $2.4<\mu_T<\mu_{\text{crit}}$. Here, $\mu_T>2.4$ is required in order for the reference state to exhibit reversal, while $\mu_{\text{crit}}=3.11$ is Taylor's critical value for the onset of minimum energy helical states. We postulate two small departures from this reference state. The first concerns the presence of a feeble pressure gradient, resulting from central joule heating of the discharge. This, in principle, accounts for the presence of a wide spectrum of g-modes, saturated at small amplitude, and dominated by the modes with $m=1$, since these harmonics will tend to have the least stabilizing values of the tearing index Δ'. For the second departure from a Taylor state we model peaking of the plasma current in the core with a step in the value of μ, so that

$$\begin{aligned}\mu(r) &= \mu_0, \quad 0 \leqslant r \leqslant r_{\text{step}}, \\ &= \mu_1, \quad r_{\text{step}} < r \leqslant a,\end{aligned} \tag{1}$$

with a the plasma minor radius, $\Delta\mu=(\mu_0-\mu_1)>0$, $\mu_1<\mu_T<\mu_0$ and r_{step} chosen to be in the plasma core. We assume the presence of a perfectly conducting wall at $r=a$, i.e., no vacuum is included between $r=a$ and the wall. We parameterize this family of equilibria in terms of the quantity $\Delta\mu$, which measures the degree of current peaking, and specify the pair (μ_0,μ_1) in terms of the initial value in the Taylor state, μ_T, by constraining the equilibria to have evolved from the reference Taylor state while conserving toroidal flux and the total plasma current, I_p. We then calculate the stability indices, i.e., values of Δ', for all the relevant tearing modes, as a function of the inhomogeneity parameter $\Delta\mu$. Qualitatively speaking, increasing values of $\Delta\mu$ should correspond to increasing time, so that the resulting figures can be loosely interpreted in terms of time evolution.

What emerges is a simple picture in which one tearing mode (in fact, the one whose mode rational surface is located at smaller radius than the step in μ) is driven unstable as the magnitude of the step increases, while the stability indices of all other tearing modes become progressively more negative (stabilizing). If we assume an expression for mode saturation of the form

$$r_s\Delta' = \alpha W - \frac{\beta}{W}, \tag{2}$$

where $W=w/r_s$ with w the island width, r_s is the resonance radius of the mode under consideration, α is a numerical constant, and β is a small, numerical coefficient, proportional to the local pressure gradient, then the amplitudes of all the weak, pressure driven, g-modes should decrease as the inhomogeneity, $\Delta\mu$, increases, while one (core resonant) mode is driven to large amplitude as its stability index, Δ', first becomes positive and then large. We speculate that, as a critical $\Delta\mu$ is reached, the plasma relaxes back to a Taylor-type equilibrium with constant μ and a cyclic behavior is established.

It is not immediately clear that Eq. (2) can be justified for a RFP in which dynamo action is present, but this form does arise naturally[22] in tokamaks where the term proportional to β has the opposite sign, if the bootstrap current is neglected, and has the same sign as above for the neoclassical tearing modes (NTMs).[23,24]

This paper is organized as follows: In Sec. II we describe these equilibria in more detail and explore some natural constraints on $\Delta\mu$ arising from a monotonicity condition for $q(r)$. In Sec. III we describe the linear stability calculations and present the results. A summary and conclusions are presented in Sec. IV. Appendices A and B are devoted to details of the Δ' calculation and to ideal MHD stability considerations, respectively.

II. FORCE-FREE EQUILIBRIA WITH STEPPED-μ PROFILE

In his classical paper[3] Taylor conjectured that the relaxation process occurring in toroidal pinches with perfectly conducting boundaries leads to a force-free state in which the magnetic field **B** satisfies the condition

$$\nabla \times \mathbf{B} = \mu \mathbf{B}, \tag{3}$$

where μ is a constant. Such result derives from assuming that the relaxation process tends to bring the system into a state of minimum magnetic energy under the constraints of the conservation of global helicity and toroidal magnetic flux. Let us consider the cylindrical approximation of a torus and consequently the relaxation process occurring in a plasma contained in a cylindrical domain of radius a and length $2\pi R$, equipped with a system of coordinates (r,θ,z), where r, θ, and z indicate the distance from the axis of the cylinder, the poloidal angle and the distance parallel to the cylindrical axis, respectively. We also consider distances normalized with respect to a, i.e., $\hat{r}=r/a$, $\hat{\mu}=\mu/a$ (hats will be dropped for simplicity). In the axisymmetric case, Eq. (3) admits the well-known Bessel function model (BFM) solutions

$$B_r = 0, \quad B_\theta = B_0 J_1(\mu r), \quad B_z = B_0 J_0(\mu r), \tag{4}$$

where B_0 is a constant denoting the amplitude of the field. If $\mu > 2.404$, B_z becomes negative inside the chamber accounting for the experimentally observed reversal of the toroidal field. On the other hand, according to Taylor's theory, the value of μ for minimum energy states cannot be greater than 3.11. In particular, if one defines a normalized global helicity $\hat{K}=(K/\phi^2)(a/R)$, where K is the dimensional global helicity and ϕ is the toroidal flux, then it can be shown that for $2.4 < \hat{K} \leq 8.21$ the minimum energy states are reversed, cylindrically symmetric states with $2.4 \leq \mu < 3.11$, whereas if $\hat{K} > 8.21$ the minimum energy states are a linear combination of a cylindrically symmetric part and a helically symmetric part, with the value of μ fixed at 3.11. The value $\mu=3.11$ corresponds also to the threshold at which the BFM (4) becomes tearing unstable.[4] The magnetic surfaces where the tearing instability can develop are those identified by the resonance condition $q(r)=(rB_z/RB_\theta)=m/n$, where m and n are integers corresponding to the poloidal and toroidal mode numbers, respectively. For the BFM equilibrium the resonance condition reads

$$\frac{J_0(\mu r)}{J_1(\mu r)} r = -\frac{m}{k}, \tag{5}$$

where $k=-n/R$ is the toroidal wave number of the perturbation. The analysis of Gibson and Whiteman[4] shows that, when increasing the value of μ up to 3.11, the first helical mode to become unstable resonates in the reversal region, near the edge of the plasma ($r \approx 0.974$). This corresponds to a ($m=1$, $k=1.25$) mode. The linear stability properties of a force-free equilibrium will, however, be different if the profile of the function μ is modified. Indeed, experiments do reveal that the μ profile in RFPs is not exactly flat. We will show that, if we choose μ as a decreasing function of r, e.g., a downward step-function, the stability properties of the resulting force-free equilibrium will be such that the most unstable mode can have mode numbers corresponding to those that dominate the magnetic spectrum during QSH states. In other words, the introduction of a jump in the profile of μ will make it possible to destabilize the mode of interest while keeping all the other modes stable. Although the choice of a step-function for μ corresponds to a highly idealized case, it possesses the advantage that a fully analytical treatment of the problem is possible and lays the basis for later investigations of more refined and realistic models that will require, however, a numerical approach. Let us consider, then, a cylindrically symmetric equilibrium field **B** satisfying Eq. (3) with $\mu=\mu(r)$ defined in the following way:

$$\mu(r) = \begin{cases} \mu_0 & \text{if } 0 \leq r \leq r_{\text{step}}, \\ \mu_1 & \text{if } r_{\text{step}} < r \leq 1, \end{cases} \tag{6}$$

where μ_0, μ_1, and r_{step} are constant and $\mu_0 > \mu_1$ in order to have a decreasing μ profile, as suggested by experiments. Criteria to constrain the values of μ_0, μ_1, and r_{step} will be given below.

Solving Eq. (3) separately in the two regions $0 \leq r \leq r_{\text{step}}$ and $r_{\text{step}} < r \leq 1$ yields

$$B_r = 0,$$

$$B_\theta = \begin{cases} \bar{a} J_1(\mu_0 r) + \bar{b} Y_1(\mu_0 r) & \text{if } 0 \leq r \leq r_{\text{step}}, \\ \bar{c} J_1(\mu_1 r) + \bar{d} Y_1(\mu_1 r) & \text{if } r_{\text{step}} < r \leq 1, \end{cases} \tag{7}$$

$$B_z = \begin{cases} \bar{a} J_0(\mu_0 r) + \bar{b} Y_0(\mu_0 r) & \text{if } 0 \leqslant r \leqslant r_{\text{step}}, \\ \bar{c} J_0(\mu_1 r) + \bar{d} Y_0(\mu_1 r) & \text{if } r_{\text{step}} < r \leqslant 1, \end{cases}$$

where $\bar{a}$, $\bar{b}$, $\bar{c}$, and $\bar{d}$ are arbitrary constants to be determined. The requirement of boundedness of **B** at $r=0$ implies $\bar{b}=0$. The constant $\bar{a}$ can be set equal to some chosen value B_0 corresponding to the amplitude of the field in the region to the left of the step. The constants $\bar{c}$ and $\bar{d}$ are determined by imposing the continuity of the equilibrium field at r_{step}. This means that $\bar{c}$ and $\bar{d}$ must be such that

$$B_0 J_1(\mu_0 r_{\text{step}}) = \bar{c} J_1(\mu_1 r_{\text{step}}) + \bar{d} Y_1(\mu_1 r_{\text{step}}),$$

$$B_0 J_0(\mu_0 r_{\text{step}}) = \bar{c} J_0(\mu_1 r_{\text{step}}) + \bar{d} Y_0(\mu_1 r_{\text{step}}). \tag{8}$$

Using the Wronskian relation

$$Y_0(x) J_1(x) - Y_1(x) J_0(x) = \frac{2}{\pi x}, \tag{9}$$

one can express the solutions of Eq. (8) in the following way:

$$\bar{c} = \frac{\pi}{2} B_0 \mu_1 r_{\text{step}} [J_1(\mu_0 r_{\text{step}}) Y_0(\mu_1 r_{\text{step}}) - Y_1(\mu_1 r_{\text{step}}) J_0(\mu_0 r_{\text{step}})], \tag{10}$$

$$\bar{d} = \frac{\pi}{2} B_0 \mu_1 r_{\text{step}} [J_1(\mu_1 r_{\text{step}}) J_0(\mu_0 r_{\text{step}}) - J_1(\mu_0 r_{\text{step}}) J_0(\mu_1 r_{\text{step}})]. \tag{11}$$

We can now construct equilibria depending only on the parameters B_0, μ_0, μ_1, and r_{step}, subject to the following constraints. First of all, we consider a reference Taylor state, corresponding to the BFM solution with $\mu=\mu_T=$constant and $2.4<\mu_T<3.11$. This Taylor state will have prescribed values of helicity, toroidal flux, ϕ, and consequently of total current along the z-direction, I_z. We will constrain the values of B_0, μ_0, μ_1 so that the resulting stepped-μ equilibria will have the same values of ϕ and I_z of the reference Taylor state. More exactly the following relations will have to be satisfied:

$$\phi = 2\pi \frac{B_T}{\mu_T} J_1(\mu_T) = 2\pi \left(- B_0 r_{\text{step}} J_1(\mu_0 r_{\text{step}}) \frac{\Delta\mu}{(\mu_0 - \Delta\mu)\mu_0} + \frac{1}{\mu_0 - \Delta\mu} [\bar{c} J_1(\mu_0 - \Delta\mu) + \bar{d} Y_1(\mu_0 - \Delta\mu)] \right), \tag{12}$$

$$I_z = 2\pi B_T J_1(\mu_T) = 2\pi [\bar{c} J_1(\mu_0 - \Delta\mu) + \bar{d} Y_1(\mu_0 - \Delta\mu)]. \tag{13}$$

Equations (12) and (13) express the conservation of toroidal flux and total current, respectively. This will leave us with a family of solutions parametrized by r_{step} and $\Delta\mu=(\mu_0-\mu_1)>0$, with $\mu_1<\mu_T<\mu_0$. Finally, we impose that, for each equilibrium belonging to such a family the corresponding winding number $q(r)$, be a monotonically decreasing function. This will prevent the appearance of double resonances. It can be seen that a good indication of the monotonicity of $q(r)$ is the local condition

$$\left. \frac{dq}{dr} \right|_{r=r_{\text{step}}^+} < 0, \tag{14}$$

which for the considered equilibria reads

$$\mu_1 > 2 \frac{J_0(\mu_0 r_{\text{step}}) J_1(\mu_0 r_{\text{step}})}{r_{\text{step}} [J_0^2(\mu_0 r_{\text{step}}) + J_1^2(\mu_0 r_{\text{step}})]}. \tag{15}$$

This sets therefore a lower bound for μ_1, for given μ_0 and r_{step}. As mentioned in Sec. I, the departure from a Taylor cylindrical state consists of an evolution through a sequence of stepped-μ equilibria of the form described above. We assume, for the sake of simplicity, that r_{step} does not vary during this evolution. Starting from a reversed tearing stable Taylor state, corresponding to $\Delta\mu=0$ and $\mu_T<3.11$, the system tends to depart from it on resistive time scales due to plasma heating and resistive diffusion. We model this through the formation of a step in μ with positive $\Delta\mu$. Initially, for very small values of $\Delta\mu$, the system is still stable, but as $\Delta\mu$ increases with time, the instability threshold for tearing modes is crossed and a magnetic island forms in the plasma core, between r_{step} and the magnetic axis, as will be shown in the next section. From a linear stability point of view, the system proceeds toward states with a steeper and steeper step, corresponding to a larger and larger growth rate (larger values of Δ') for the tearing mode with dominant helicity.

In Fig. 1, one can see three different $q(r)$ profiles corresponding to three different equilibria reached during one evolution from an initial Taylor state.

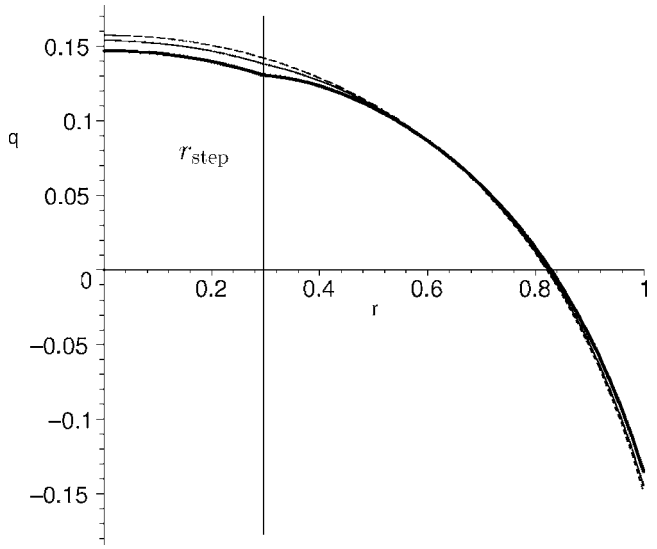

FIG. 1. Safety profile for three stepped-μ equilibria corresponding to $\Delta\mu=0$ (dashed line), $\Delta\mu=0.1$ (solid line), and $\Delta\mu=0.3$ (thick solid line). The three profiles belong to the same family of equilibria originated by an initial Taylor state characterized by $B_T/B_0=0.93$ and $\mu_T=2.93$.

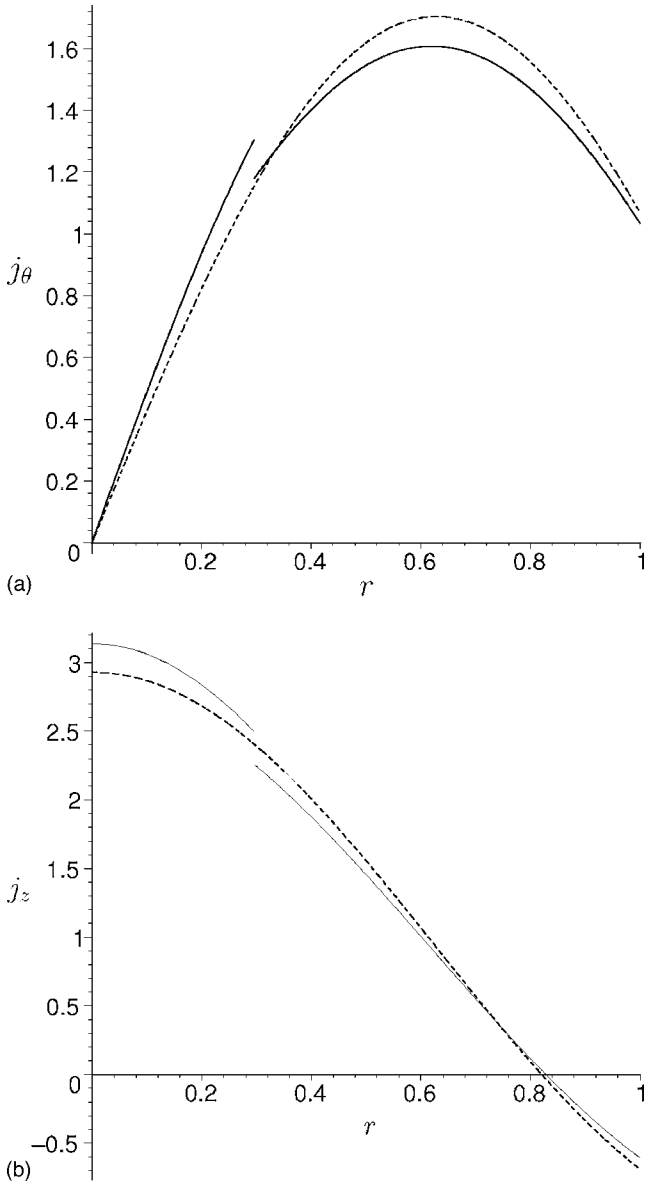

FIG. 2. Comparison between current density profiles of a stepped-μ equilibrium (solid line) with $\Delta\mu=0.3$ and of the corresponding initial Taylor state (dashed line) characterized by $\mu_T=2.93$ and $B_T/B_0=0.93$. (a) refers to the poloidal component of j, whereas (b) refers to the toroidal component.

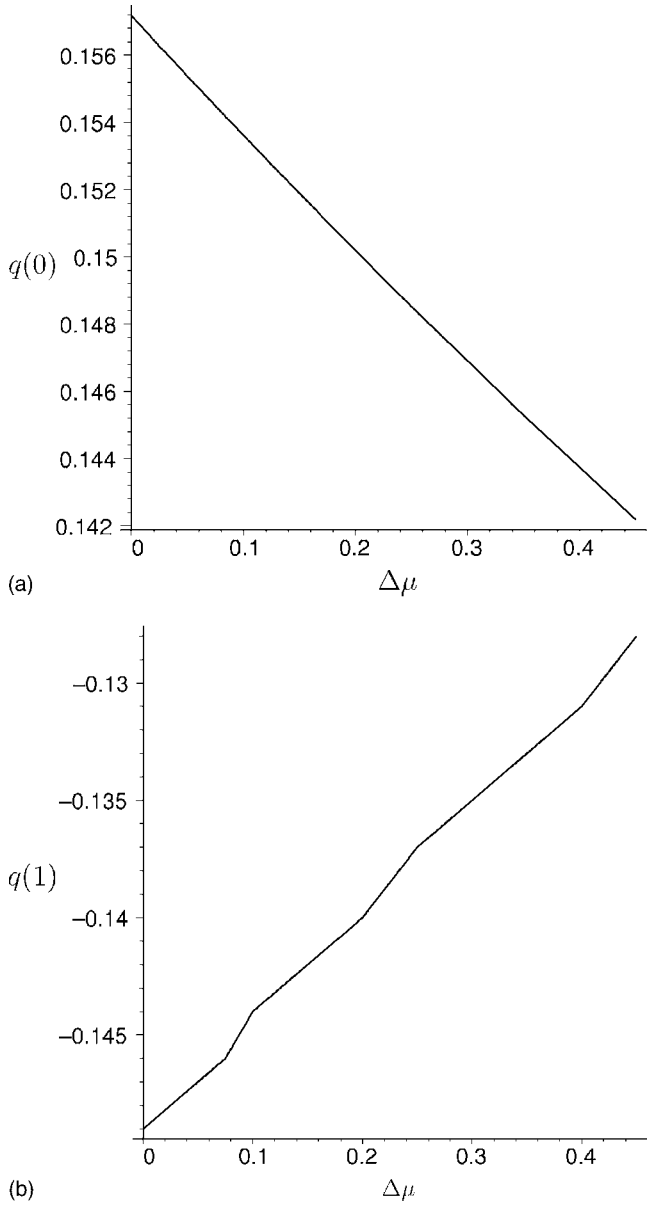

FIG. 3. (a), (b) Values of $q(0)$ and $q(1)$, respectively, as functions of $\Delta\mu$ during an evolution from an initial Taylor state with $B_T/B_0=0.93$ and $\mu_T=2.93$.

Figure 2 shows the comparison between the current density profiles of a stepped-μ equilibrium reached during the evolution and the profiles for the corresponding initial Taylor state. It is also interesting to consider in particular the evolution of the values of q at the center and at the edge of the cylinder as $\Delta\mu$ increases. In particular, expanding q about $r=0$ yields that in the vicinity of $r=0$ q is equal to $2/R\mu_0$ to leading order.

Therefore, the value of q near the center decreases as $\Delta\mu$ increases, as shown in Fig. 3. The behavior of q at the edge is shown in Fig. 3(b). The plot shows that as the state evolves through the series of stepped-μ equilibria the toroidal field gets less and less reversed. This behavior naturally agrees with the idea that the system tends to depart from the reversed Taylor state, which is incompatible with Ohm's law.[14,18,25] The tendency toward a less reversed state might reflect the attempt of the system to access a stationary nonreversed state, which would resolve the incompatibility with Ohm's law on resistive time scales. Moreover, it is important to point out that the behaviors of q near the center and near the edge during the departure phase qualitatively correspond to the tendencies of the values $q(0)$ and $q(a)$ observed experimentally during the ramp phase of a QSH.[20]

Among the equilibria thus generated, we can find one which is linearly unstable with respect to perturbations with a given helicity, but stable with respect to all the other modes. This equilibrium can be reached as $\Delta\mu$ increases in time, triggering the formation of a QSH state. Given the above conditions, the construction of a specific example of such an equilibrium proceeds in the following way. First one chooses the value of the effective aspect ratio of interest, R/a. Then one chooses the value of μ_0. This choice is also

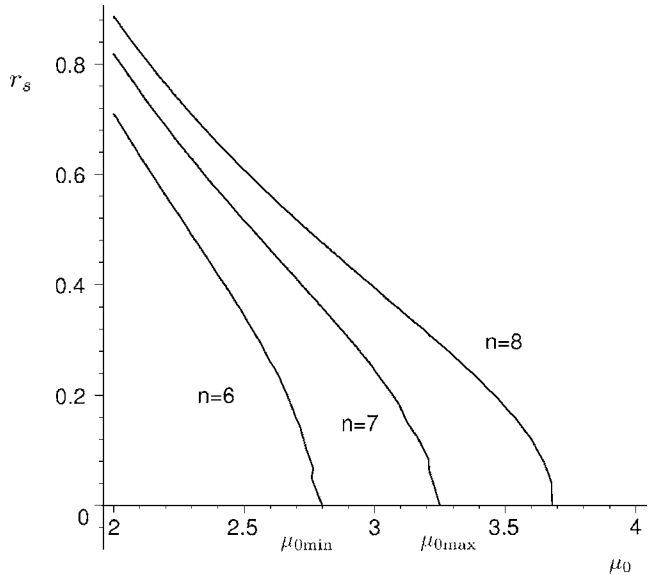

FIG. 4. The figure shows the relations, as given by the formula (16), between the resonance radii r_s and the values of μ_0 for the modes (1,6), (1,7), and (1,8), assuming $\bar{n}=7$. The aspect ratio is equal to 4.34. The intersections of the curves for $n=6$ and $n=7$ with $r_s=0$ determine the minimum and maximum admissible values of μ_0, respectively, in order to have a resonance with the mode (1,7) and to exclude the resonance with modes with $m=1$ and $n<7$.

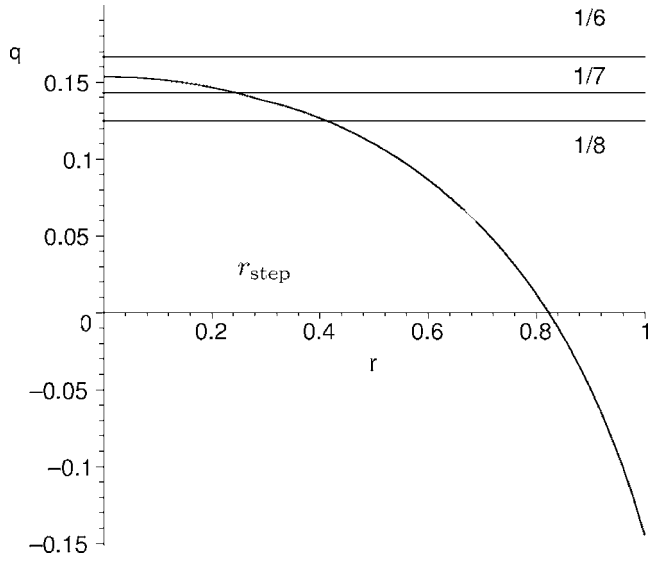

FIG. 5. The plot shows an example of safety profile q for a stepped-μ equilibrium, near marginal stability, with $\mu_0=3$, $\mu_1=2.9$, $r_{\text{step}}=0.296$, and $R=4.34$. This equilibrium resonates to the right of the step with the mode (1,8), inside the step with the mode (1,7) and does not resonate with the mode (1,6).

subject to restrictions. In fact, if we aim at destabilizing a particular mode, that we can denote as $(m=1,\bar{n})$ (considerations on $m>1$ modes, which typically possess a lower growth rate, will be made in the next section), such mode must of course resonate inside the plasma. Moreover, as we already pointed out, the dominant mode in QSH states resonate in the nonreversed region. Finally, it is also desirable to prevent the modes with $n<\bar{n}$ from resonating inside the plasma, since such modes are not relevant during QSH states. Therefore, the parameter μ_0 must be chosen in such a way that the resonance equation for the mode $(m=1,\bar{n})$,

$$RJ_1(\mu_0 r) - \bar{n} r J_0(\mu_0 r) = 0 \tag{16}$$

has one solution for $0<r<1$ and that the equation

$$RJ_1(\mu_0 r) - (\bar{n}-1) r J_0(\mu_0 r) = 0 \tag{17}$$

has no solution for $0<r<1$. The latter condition is of course sufficient to make sure that all the modes with $n<\bar{n}$ do not resonate inside the plasma. Notice also that, given that the value of q near the center decreases as $\Delta\mu$ increases, as shown in Fig. 3, it is excluded that the modes with $m=1$ and $n<\bar{n}$ could become resonant at later stages of the departure phase. In Eqs. (16) and (17) we used the expression for the magnetic equilibrium valid for $0<r<r_{\text{step}}$. This is because, as it will be shown, the desired effect on the stability properties of the equilibrium occurs if the step is located to the right of the resonant radius of the mode $(1,\bar{n})$ and to the left of the resonance of the mode $(1,\bar{n}+1)$.

An example of how the minimum and maximum values for μ_0 are determined is shown in Fig. 4.

Once μ_0 is fixed, one can then choose a value for r_{step} such that

$$r_{s\bar{n}} < r_{\text{step}} < r_{s(\bar{n}+1)}, \tag{18}$$

where $r_{s\bar{n}}$ and $r_{s(\bar{n}+1)}$ indicate the resonance radii of the modes $(1,\bar{n})$ and $(1,\bar{n}+1)$, respectively.

We are also reminded that μ_1, μ_0, and r_{step} have to satisfy the restrictions above, i.e.,

$$2\frac{J_0(\mu_0 r_{\text{step}})J_1(\mu_0 r_{\text{step}})}{r_{\text{step}}[J_0^2(\mu_0 r_{\text{step}}) + J_1^2(\mu_0 r_{\text{step}})]} < \mu_1 < \mu_0. \tag{19}$$

On the other hand, the value of B_0 is determined from the flux conservation condition (12).

Once μ_0, μ_1, r_{step}, and B_0 are fixed, the construction of the equilibrium is completed. One only has to check that the z component of the equilibrium field so obtained reverses near the edge.

An example of the $q(r)$ profile for a stepped-μ force-free field is shown in Fig. 5. This example refers in particular to the values $R=4.34$ and $\bar{n}=7$, which are characteristic of QSH states in the RFX experiment.[26]

III. LINEAR STABILITY

In this section, we are going to show that the stepped-μ equilibria defined in Sec. II can be linearly unstable to a single $(m=1,n)$ mode, with n corresponding to central resonance. Thus, it would be natural to interpret the saturated magnetic island arising from this mode as corresponding to the dominant magnetic helical structure observed in QSH experiments. The core of the analysis consists of deriving and studying the expression for the tearing stability parameter, Δ', whose sign determines the stability of the equilibrium with respect to a given perturbation.[6] For a given resonant radius r_s, where $q(r_s)=m/n$, Δ' is defined as

$$\Delta' = \frac{1}{\tilde{\chi}_0}\left(\left.\frac{d\tilde{\chi}}{dr}\right|_{r_s^+} - \left.\frac{d\tilde{\chi}}{dr}\right|_{r_s^-} \right) \tag{20}$$

where $\tilde{\chi}(r)$ represents the amplitude of the linear perturbation $\tilde{\chi}(r)=m\tilde{B}_z(r)-kr\tilde{B}_\theta(r)$, of the helical flux function in the outer region and $\tilde{\chi}_0$ is the value of $\tilde{\chi}$ at r_s (throughout the paper we make use of the symbol $\sim$ to denote a perturbation).

Our starting point for determining the function $\tilde{\chi}$ is the set of magnetohydrodynamics equations,

$$\rho\left(\frac{\partial \mathbf{v}}{\partial t} + \mathbf{v}\cdot\nabla\mathbf{v}\right) = \mathbf{j}\times\mathbf{B} - \nabla p, \tag{21}$$

$$\mathbf{E} + \mathbf{v}\times\mathbf{B} = \eta\mathbf{j}, \tag{22}$$

supplemented by the incompressibility condition, $\nabla\cdot\mathbf{v}=0$. In the equation of motion (21), ρ represents the mass density, $\mathbf{v}$ is the plasma velocity, and p is the plasma pressure. In Ohm's law (22), we indicate with $\mathbf{E}$, the electric field, and with η the resistivity, which is taken to be constant. We assume that, at equilibrium, the magnetic field is a cylindrically symmetric force-free field of the form (7), while the plasma pressure and velocity are zero. This actually corresponds to a quasiequilibrium, in the sense that the resulting equilibrium electric field, which obeys Ohm's law, is not curl-free, but it evolves on the slow, resistive diffusion time scale.

We consider a helical perturbation of such equilibrium. Following the standard linear theory of tearing modes,[6] we separate the domain into two regions. We consider an inner region, centered around a surface that is resonant with perturbations of a given helicity, and an outer region, complementary to the inner region, where the effects of resistivity are negligible and an ideal Ohm's law is appropriate. The determination of the parameter Δ' is based solely on the knowledge of the solutions for $\tilde{\chi}$ in the outer region. It is convenient to introduce the following representation for the magnetic and velocity fields. Let us consider two integers m and n and define the helical coordinate $u=m\theta+kz$, where m and $k=-n/R$ represent poloidal and toroidal wave numbers, respectively. A divergence-free field $\mathbf{B}$ spatially depending only on r and u (i.e., helically symmetric), can be expressed as

$$\mathbf{B}(r,u) = \nabla\chi(r,u)\times\mathbf{h} + g(r,u)\mathbf{h}, \tag{23}$$

where χ is the helical flux and g is called the helical field.[18] The vector $\mathbf{h}$ is defined as $\mathbf{h}=f(r)\nabla r\times\nabla u$, where $f(r)=r/(m^2+k^2r^2)$ is a metric term. Similarly, for an incompressible velocity field, we can write

$$\mathbf{v}(r,u) = \nabla\varphi(r,u)\times\mathbf{h} + v_h(r,u)\mathbf{h}. \tag{24}$$

As anticipated above, we look for helically symmetric solutions for the magnetic field and for the velocity field given by the superposition of a cylindrically symmetric equilibrium and of a helical, time-dependent perturbation. Thus, the magnetic field can be expressed as in Eq. (23), with

$$\begin{aligned}\chi(r,u,t) &= \chi_{\mathrm{eq}}(r) + \tilde{\chi}(r)e^{\gamma t+iu},\\ g(r,u,t) &= g_{\mathrm{eq}}(r) + \tilde{g}(r)e^{\gamma t+iu}.\end{aligned} \tag{25}$$

The subscript eq refers to equilibrium quantities, whereas γ is the growth rate of the perturbations $\tilde{\chi}$ and $\tilde{g}$. It is easy to show that, in terms of the flux function, the resonant surfaces are those satisfying the condition $d\chi_{\mathrm{eq}}/dr=0$. Similarly, we assume

$$\varphi(r,u) = \tilde{\varphi}(r)\mathrm{e}^{\gamma t+iu}, \quad v_h(r,u) = \tilde{v_h}(r)\mathrm{e}^{\gamma t+iu}. \tag{26}$$

We expect that a nonzero equilibrium flow will introduce only a negligible correction to the calculation of the tearing stability index, providing that the equilibrium flow velocity is smaller than the Alfvèn velocity. On the other hand, an equilibrium flow may modify the perturbed equations within the resonant layer, hence affecting the stability of tearing modes. However, only relatively large sheared flows would produce an important effect. Likewise, compressibility effects are expected to be negligible for the linear stability calculations, although they may play a role for the determination of the nonlinear saturation level.[27]

Let us consider first the equation of motion (21). We assume that pressure perturbations are negligibly small. Then, for small perturbations, we can insert the ansatz (25) and (26) into the linearized equation of motion. On the time scale of the linear growth of the instability, the contributions to the linearized equation coming from the velocity field are negligible as compared to the terms coming from the Lorentz force. The projections of the linearized equation of motion along $\mathbf{h}$ and along ∇r (or equivalently along ∇u) then yield

$$\tilde{g} = \frac{g'_{\mathrm{eq}}}{\chi'_{\mathrm{eq}}}\tilde{\chi} \tag{27}$$

and

$$\frac{d^2\tilde{\chi}}{dr^2} + \frac{1}{f}\frac{df}{dr}\frac{d\tilde{\chi}}{dr} + \left[\left(\frac{g'_{\mathrm{eq}}}{\chi'_{\mathrm{eq}}}\right)^2 - \frac{1}{rf} + \frac{g_{\mathrm{eq}}}{\chi'_{\mathrm{eq}}}\left(\frac{g'_{\mathrm{eq}}}{\chi'_{\mathrm{eq}}}\right)' - \beta\frac{g'_{\mathrm{eq}}}{\chi'_{\mathrm{eq}}}\right]\tilde{\chi} = 0, \tag{28}$$

respectively. In Eqs. (27) and (28), the symbol $'$ indicates derivative with respect to r, whereas $\beta(r)=-2mk/(m^2+k^2r^2)$. After $\tilde{\chi}$ is obtained as the solution of Eq. (28), $\tilde{g}$ follows straightforwardly from Eq. (27). The fields $\tilde{\varphi}$ and $\tilde{v}_h$ are enslaved variables and can be recovered from the linearized Ohm's law, Eq. (22), where $\eta=0$ is set to zero.

For our equilibrium field the relation $\mu=g'_{\mathrm{eq}}/\chi'_{\mathrm{eq}}$ holds and Eq. (28) can be written as

$$\tilde{\chi}' + \frac{f'}{f}\tilde{\chi}' + \left(\mu^2 - \frac{1}{rf} + \frac{g_{\mathrm{eq}}}{\chi'_{\mathrm{eq}}}\mu' - \beta\mu\right)\tilde{\chi} = 0. \tag{29}$$

The choice of μ as a step function implies that the term $(g_{eq}/\chi'_{eq})\mu'$ vanishes everywhere except at $r=r_{step}$, where it becomes singular. However, this singularity is an artifact of the stepped-μ equilibrium and it does not significantly affect the linear stability results, as long as r_s is sufficiently far from r_{step}. Notice that if $\mu_0=\mu_1$ the equation reduces to the one derived in Ref. 28 for a Taylor equilibrium. The requirement of boundedness at $r=0$ and the assumption of perfectly conducting wall, in the absence of a vacuum region, imply that $\tilde{\chi}$ must satisfy the boundary conditions

$$\tilde{\chi}(0)=\bar{\chi}, \tag{30}$$

with $\bar{\chi}$ equal to a (arbitrary) constant value, and

$$\tilde{\chi}(1)=0. \tag{31}$$

The presence of a resonant radius r_s between $r=0$ and $r=1$ implies that the equation must be solved separately in the two regions, $0\leqslant r<r_s$ and $r_s<r\leqslant 1$. Let us consider the case in which r_s lies between 0 and r_{step} (the case $r_{step}<r_s<1$ can be treated in an analogous way). Furthermore, let us focus first on the case $m=1$, which is the most directly relevant for QSH states (further details on the derivation of Δ' for $m\neq 1$ can be found in Appendix A). The solution of Eq. (29) then reads

$$\tilde{\chi}=\begin{cases} kz_0[\delta_1 J_0(z_0)-\lambda_1 Y_0(z_0)]+(\mu_0-k)[\delta_1 J_1(z_0)-\lambda_1 Y_1(z_0)] & \text{if } 0<z_0<z_s, \\ kz_0[\delta_2 J_0(z_0)-\lambda_2 Y_0(z_0)]+(\mu_0-k)[\delta_2 J_1(z_0)-\lambda_2 Y_1(z_0)] & \text{if } z_s<z_0<z_{step^-}, \\ kz_1[\delta_3 J_0(z_1)-\lambda_3 Y_0(z_1)]+(\mu_1-k)[\delta_3 J_1(z_1)-\lambda_3 Y_1(z_1)] & \text{if } z_{step^+}<z_1<z_a, \end{cases} \tag{32}$$

where we introduced the variables $z_0=\sqrt{\mu_0^2-k^2}r$, $z_1=\sqrt{\mu_1^2-k^2}r$, $z_s=\sqrt{\mu_0^2-k^2}r_s$, $z_a=\sqrt{\mu_1^2-k^2}$, $z_{step^-}=\sqrt{\mu_0^2-k^2}r_{step}$, $z_{step^+}=\sqrt{\mu_1^2-k^2}r_{step}$ and where δ_i, λ_i, with $i=1,2,3$, represent arbitrary constants. The condition (30) implies $\lambda_1=0$ and $\bar{\chi}=0$, whereas from Eq. (31) one obtains

$$\lambda_3=\delta_3\frac{kz_aJ_0(z_a)+(\mu_1-k)J_1(z_a)}{kz_aY_0(z_a)+(\mu_1-k)Y_1(z_a)}. \tag{33}$$

The constants δ_2 and δ_3 can in principle be fixed by requiring the continuity of $\tilde{\chi}$ at r_s and at r_{step}. However, the quantity Δ' turns out to not depend on the value of these two constants. Therefore, for the sake of simplicity, we can set them equal to unity. The quantity Δ' is also insensitive to the value of δ_1 and therefore we can set $\delta_1=1$. The constant λ_2, on the other hand, has to be determined, and this can be done using the constraint

$$r_{step}\left(\frac{1}{\tilde{\chi}}\left.\frac{d\tilde{\chi}}{dz_1}\right|_{z_1=z_{step^+}}-\frac{1}{\tilde{\chi}}\left.\frac{d\tilde{\chi}}{dz_0}\right|_{z_0=z_{step^-}}\right)=G(\mu_0,\mu_1,r_{step},k). \tag{34}$$

The condition (34) expresses the jump in the logarithmic derivative of $\tilde{\chi}$ across r_{step}. The function G, which is a known quantity, can be derived from Eq. (29). The derivation can be found in Appendix A, as well as the expression for λ_2 resulting from Eq. (34). We find

$$G(\mu_0,\mu_1,r_{step},k)=(\mu_1-\mu_0)r_{step}\frac{J_0(\mu_0 r_{step})-kr_{step}J_1(\mu_0 r_{step})}{J_1(\mu_0 r_{step})+kr_{step}J_0(\mu_0 r_{step})}. \tag{35}$$

After all the arbitrary constants are fixed, the required solution for $\tilde{\chi}$ is determined and one can make use of the definition (20) to obtain the expression for Δ'. This turns out to be

$$\begin{aligned} r_s\Delta' &= \frac{z_s}{\tilde{\chi}(z_s)}\left(\left.\frac{d\tilde{\chi}}{dz_0}\right|_{z_0=z_{s^+}}-\frac{1}{\tilde{\chi}}\left.\frac{d\tilde{\chi}}{dz_0}\right|_{z_0=z_{s^-}}\right) \\ &= -\frac{2}{\pi}\lambda_2\frac{(\mu_0^2-k^2)(1+k^2r_s^2)}{G_{0J}(G_{0J}-\lambda_2 G_{0Y})}, \end{aligned} \tag{36}$$

where

$$\begin{aligned} G_{0J}(z_0) &= kz_0J_0(z_0)+(\mu_0-k)J_1(z_0), \\ G_{0Y}(z_0) &= kz_0Y_0(z_0)+(\mu_0-k)Y_1(z_0). \end{aligned} \tag{37}$$

Notice that in the case $\mu_0=\mu_1$, the marginal stability condition $\Delta'=0$ reduces to the condition $kz_aJ_0(z_a)+(\mu_0-k)J_1(z_a)=0$ derived in Ref. 4. The derivation of the expression for Δ' in the case $r_{step}<r_s<1$ proceeds in a similar way, as shown in Appendix A. The final result is

$$r_s\Delta'(r_s;\mu_0,\mu_1,r_{step})=\begin{cases} -\frac{2}{\pi}\lambda_2\frac{[\mu_0^2-k^2(r_s)][1+k^2(r_s)r_s^2]}{G_{0J}(G_{0J}-\lambda_2 G_{0Y})} & \text{if } 0<r_s<r_{step}, \\ -\frac{2}{\pi}(\lambda_3-\lambda_2)\frac{[\mu_1^2-k^2(r_s)][1+k^2(r_s)r_s^2]}{G_{1J}-\lambda_3 G_{1Y}(G_{1J}-\lambda_2 G_{1Y})} & \text{if } r_{step}<r_s<1, \end{cases} \tag{38}$$

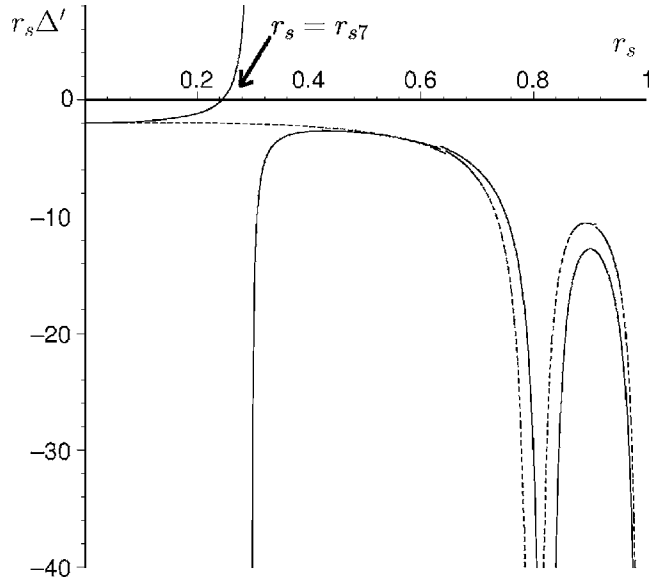

FIG. 6. Plot comparing the stability parameter $r_s\Delta'$ as a function of r_s for a Taylor (dashed line) and stepped-μ (solid line) equilibrium for modes with $m=1$. The presence of the step destabilizes the modes resonating to the left of the step while keeping the other modes stable. In particular, for the aspect ratio under consideration, i.e., $R=4.34$, the mode (1,7) resonates at $r=r_{s7}=0.246$ and the corresponding value of $r_s\Delta'$ is equal to 0.12, i.e., just above the marginal stability condition. The values of the parameters are those of Fig. 5.

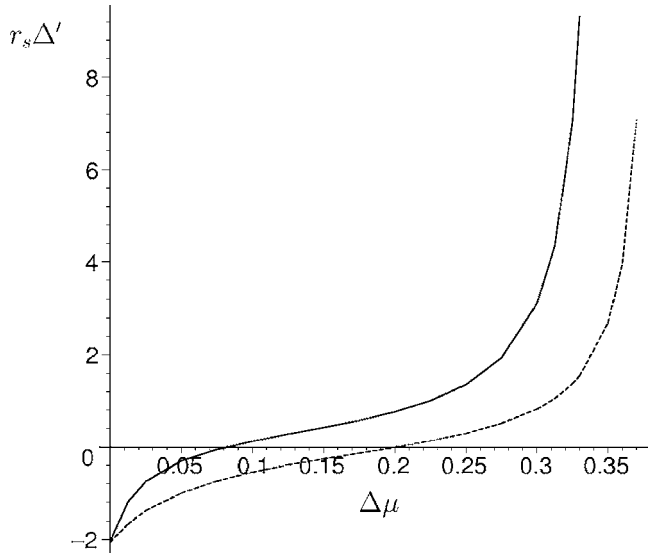

FIG. 7. The plot shows the dependence of the stability parameter Δ' on $\Delta\mu$ for $r_{\text{step}}=0.296$ (solid line) and $r_{\text{step}}=0.31$ (dashed line). The mode $(m=1, \bar{n}=7)$ in both cases resonates at $r=0.246$. Increasing the distance of the step from $r_{s\bar{n}}$ results in a higher value of $\Delta\mu$ required in order to make the mode $(m=1, n=\bar{n})$ unstable. In both cases the value of Δ' goes to infinity for some critical value of $\Delta\mu$.

where

$$G_{1J}(z_1) = kz_1J_0(z_1) + (\mu_1 - k)J_1(z_1),$$
$$G_{1Y}(z_1) = kz_1Y_0(z_1) + (\mu_1 - k)Y_1(z_1). \tag{39}$$

Note that k is a function of r_s through the resonance condition $q(r_s)=-1/kR$.

A graph of the function $r_s\Delta'(r_s)$ is shown in Fig. 6. It can be noticed that $r_s\Delta'(r_s)$ becomes singular at $r_s=r_{\text{step}}$. A second singularity occurs when r_s coincides with the reversal radius of the equilibrium field. Indeed, the resonance condition $k=-(m/r_s)(B_{\theta\text{eq}}/B_{z\text{eq}})$ implies that k must become infinite at the reversal radius. The comparison with the graph of Δ' for the case $\mu_0=\mu_1$ shows that indeed the presence of a step, although relatively small $[(\mu_0-\mu_1)/\mu_0=0.033$ in this example], considerably alters the stability properties of the equilibrium. As anticipated above, the step has a destabilizing effect on the modes resonating to the left of r_{step}, whereas modes with $r_{\text{step}}<r_s<1$ are stabilized.

This example indicates that the stepped-μ profile has stability properties relevant to the appearance of QSH states. For instance, for the parameters of the RFX experiment,[26] QSH states are often dominated by the $(m=1,\bar{n}=7)$ helicity.[14] When considering the aspect ratio of RFX, corresponding to $R/a=4.34$, the number of resonant radii is discretized, given that k can take only the values $-n/R$ with fixed R and integer n. The plot in Fig. 6 shows that by properly choosing the values of μ_0, μ_1, and r_{step}, it is possible to place the mode (1,7) above marginal stability, while keeping all the other resonant modes stable. The tearing instability of this equilibrium would then lead to the growth of a perturbation with helicity corresponding to the dominant mode appearing during QSH in RFX. Finally, notice that since a relatively small jump in μ was sufficient to guide the system toward a direction favorable to the formation of QSH states with the observed helicity, it is suggested that QSH states could emerge as a result of small deviations from Taylor states and not be unrelated to these.

As suggested in Sec. II, we may represent the departure from an initial Taylor state, due to plasma heating and resistive diffusion, as an evolution through a series of stepped-μ equilibria with increasing values of $\Delta\mu$. Then, it is interesting to study the variation of Δ' for the $(m=1, n=\bar{n})$ mode, as $\Delta\mu$ increases. We find that Δ', which is negative for $\Delta\mu=0$, changes sign at a first critical value in $\Delta\mu$. Interestingly, a second critical value of $\Delta\mu$ is found, at which Δ' goes to infinity.

This behavior is depicted in Fig. 7. This singularity indicates the appearance of an ideal instability. Notice also that shifting r_{step} away from $r_{s\bar{n}}$ implies that higher values of $\Delta\mu$ are required in order to make the mode $(m=1, n=\bar{n})$ tearing unstable. This reflects the fact that the destabilizing effect due to the presence of the step becomes weaker when the distance between r_{step} and $r_{s\bar{n}}$ is increased.

Figure 8 shows the plots of Δ' as a function of r_s for modes with higher poloidal mode numbers, $m=2,3,4$. It can be seen that modes with higher m are more stable with increasing m. Nevertheless there is a very small region near r_{step} where, even for $m>1$ modes, the presence of the step makes Δ' positive and actually infinite at $r=r_{\text{step}}$. However, for our choice of the aspect ratio, there are no modes with $m=2,3,4$ resonating inside this small region of instability. It could be argued that, in general, for a given aspect ratio it is in principle always possible to find a pair (m,n) such that the corresponding mode resonates arbitrarily close to r_{step} and therefore in the small region with positive Δ' so that such

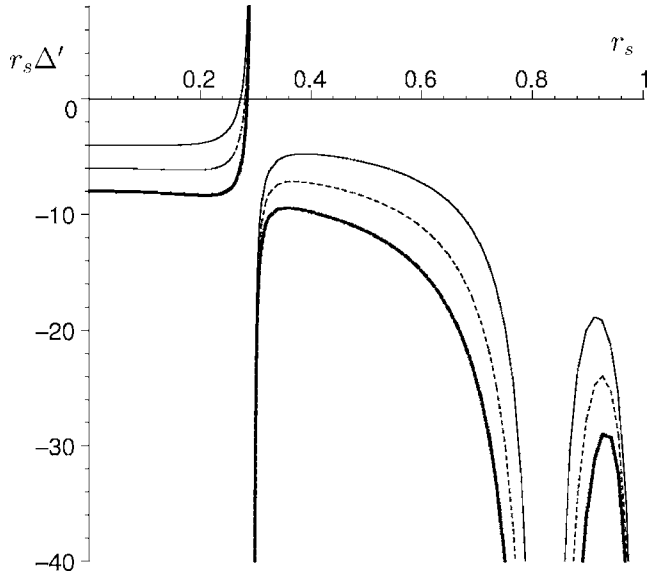

FIG. 8. The plot shows the stability parameter $r_s\Delta'$ as a function of r_s for modes with $m=2$ (solid), $m=3$ (dashed), and $m=4$ (thick). In all cases Δ' is negative over almost the entire domain, thus implying stability. The only region of potential instability is located just to the left of the step. For the given aspect ratio, however, none of the modes under consideration resonates in that region. Parameters are as in Fig. 5.

mode would indeed be unstable. However, in general this would happen for unrealistically high values of m and n. Moreover, one should bear in mind that the abrupt growth of Δ' in the vicinity of r_{step} for high m-modes is a consequence of the artifact of considering a discontinuous equilibrium μ profile. If the step were replaced by a very steep but smoother profile, the field line bending effect for high m modes would overcome the effect due to the presence of a strong gradient in the current density and this would stabilize modes resonating close to the region of rapid variation of the equilibrium current. Furthermore, finite Larmor radius effects are expected to stabilize modes with large values of m.

Finally, it is natural to ask what are the implications of the presence of a step in the μ profile with regard to ideal instabilities. Indeed, we have checked that the equilibrium considered in the above example is stable with respect to $m=1$ ideal modes. The details of this analysis are shown in Appendix B.

IV. CONCLUSIONS

In this paper, we have presented the linear stability analysis of a force-free equilibrium close to a Taylor-relaxed state against tearing modes. The departure from a reference Taylor-relaxed state, with $\mu=\mu_T=$constant, has been introduced through a step in the μ profile, where $\mu=\mathbf{J}\cdot\mathbf{B}/B^2$, cf. Eq. (1). In our intentions, this stepped-μ profile should represent very schematically the peaking of the current density, starting from a Taylor-relaxed state, due to plasma heating and resistive diffusion. Thus, the amplitude of this departure, as quantified by $\Delta\mu=\mu_0-\mu_1>0$ [cf. Eq. (1)] should increase in time, until a threshold value of $\Delta\mu$ is reached, $\Delta\mu=\Delta\mu_1$, corresponding to the instability of a tearing mode, i.e., $\Delta'(\Delta\mu_1)=0$. The linear stability analysis also reveals the existence of a second threshold value, $\Delta\mu=\Delta\mu_2$, at which Δ' goes to infinity, signifying ideal instability (cf. Fig. 7). Clearly, for the Taylor relaxed state with $\Delta\mu=0$ and $\mu=\mu_T$, the tearing stability parameter Δ' is negative throughout the plasma column for relevant values of $\mu_T<3.11$. The step is localized at a radius, r_{step}, which is held fixed in our analysis. The choice of such a representation of the μ profile is motivated by reasons of simplicity, as this choice allows one to carry out a fully analytic investigation of the linear tearing mode. Preliminary numerical investigations[29] where the step in μ is smoothed out using a hyperbolic tangent profile of width δ, indicate that the analytic results for Δ' are essentially confirmed as long as $\delta\ll|r_{\text{step}}-r_s|$.

Concentrating on modes with poloidal mode number $m=1$, we have shown that the first tearing mode to become linearly unstable is the one whose resonant surface, $r=r_s$, where $q(r_s)=1/n$, lies just to the left of r_{step} (i.e., $r_s<r_{\text{step}}$), while modes that are resonant to the right of r_{step} are made more stable, in the sense that Δ' becomes more negative. Thus, if r_{step} is chosen so that there is only one resonant surface with $m=1$ to the left of it (the one we called the central resonance), then only the single $m=1$ mode resonating there is unstable for finite values of $\Delta\mu$.

A justification for placing the step just to the right of the central resonance is as follows. We may expect that transport in RFP plasmas is determined by electromagnetic fluctuations, with low mode numbers (especially $m=1$) play an important role. Resonant surfaces corresponding to low mode numbers only sparsely populate the central plasma region, and in particular no resonant surface with $m=1$ exists to the left of the central resonance (by definition). Thus, it is reasonable to expect that the effective thermal and resistive diffusion coefficients become relatively small for $r<r_s$, giving rise to a transition region, similar to a transport barrier of the type sometimes observed in tokamak discharges,[30] which do appear fairly close to (but not necessarily at) magnetic surfaces with integer q values, most commonly $q=2$ or $q=3$. At the position of the transport barrier, strong gradients for the plasma temperature and current density profiles may form. Hence, our stepped-μ profile may be considered as a rough representation of a transport barrier localized somewhat to the right of r_s. Clearly, this is conjectural to a large extent, as conclusive evidence on the possibility of the formation of an internal transport barrier in the proximity of a magnetic island is not available at present. Force-free equilibria with stepwise pressure and μ-profiles were also considered in Hole *et al.*[31] More recently stepped pressure profile equilibria in 3D configurations have been developed by Hudson *et al.*[32] whereas the ideal MHD of a two interface configuration has been investigated by Hole *et al.*[33]

The nonlinear evolution of the single unstable tearing mode we have found will be discussed in a future publication. However, following the analysis of Refs. 34–39, one may anticipate that the tearing mode will produce a saturated magnetic island of width $w\propto\Delta'$, or alternatively $w\propto\Delta\mu$, as Δ' is approximately linear in $\Delta\mu$ for small $\Delta\mu$, as shown in Fig. 7.

It is tempting to conclude that this saturated island state corresponds to the QSH state observed in RFP experiments. However, it must be stressed that this helical state is not in equilibrium in a strict sense, but only on time scales that are short as compared to the local resistive evolution time. Indeed, the whole analysis presented in this paper is based on the assumption that two well separated time scales can be identified: A fast time scale, corresponding to the time scale for the Taylor-relaxation process, as well as the time scale for the growth and saturation of the tearing mode, and a slow time scale, scaling with the local (i.e., based on r_{step}) resistive evolution of the plasma. Thus, the saturated magnetic island will continue to evolve on the slow time scale, likewise $\Delta\mu$ will continue to increase in time. This process should continue until a critical island size, or a critical value of $\Delta\mu$ between $\Delta\mu_1$ and $\Delta\mu_2$ is reached. The critical island size (or critical $\Delta\mu$) may correspond to the distance between r_{step} and r_s. For island width exceeding $r_{\mathrm{step}}-r_s$, the step in the μ profile may be removed by magnetic reconnection, thus returning the system to a Taylor-type relaxed state. Subsequent evolution will recreate a step in the μ profile, so that a cyclic process can be established. The determination of the critical $\Delta\mu$, as well as the relaxation of the q profile as a consequence of magnetic reconnection, require nonlinear considerations and will be the focus of a future publication.

What emerges is a simple picture, in which the QSH state is viewed as a relatively small, cyclic departure from a Taylor-relaxed state, with the period of this cycle determined by a fraction of the local resistive evolution time, based on r_{step}, more precisely, the time for $\Delta\mu$ to evolve from zero to the critical value. This picture is proposed as a possible interpretation of the experimental results presented in Fig. 11 of Ref. 20. Clearly, more work needs to be done in order to confirm this picture. In particular, realistic temperature and current density profiles produced by a transport code with relevant diffusion coefficients must be considered, and the complete nonlinear evolution of the resulting modes, including the modes with $m>1$, must be investigated with the help of a fully 3D nonlinear resistive MHD code.

ACKNOWLEDGMENTS

We would like to acknowledge discussions with several RFX colleagues, and in particular D. Bonfiglio, S. Cappello, D. F. Escande, P. Martin, S. Ortolani, and R. Paccagnella. This work was partly supported by the Istituto Gas Ionizzati (IGI) of the Consiglio Nazionale delle Ricerche in the framework a FIRB collaboration. This work was also partly supported by the Euratom Communities under the contract of association between EURATOM/ENEA. The views and opinions expressed herein do not necessarily reflect those of the European Commission.

APPENDIX A: DERIVATION OF THE EXPRESSION FOR Δ'

The eigenfunction $\tilde{\chi}$ is constrained by the boundary conditions (30), (31), and (34), where in the latter the jump G of the logarithmic derivative of $\tilde{\chi}$ across the step has to be determined. Such quantity can be derived in the following way. In Eq. (29), the singular term μ' becomes the dominant one around r_{step}, and so locally that equation can be approximated by

$$\tilde{\chi}'' \approx -\frac{g_{\mathrm{eq}}}{\chi'_{\mathrm{eq}}}\mu'\tilde{\chi}. \tag{A1}$$

Integrating Eq. (A1) between r^-_{step} and r^+_{step}, considering that in this infinitesimally small interval the continuous functions $\tilde{\chi}$, g_{eq} and χ'_{eq} are approximately constant when compared to μ', leads to

$$\left.\frac{d\tilde{\chi}}{dr}\right|_{r=r^+_{\mathrm{step}}} - \left.\frac{d\tilde{\chi}}{dr}\right|_{r=r^-_{\mathrm{step}}} \approx -\frac{g_{\mathrm{eq}}(r_{\mathrm{step}})}{\chi'_{\mathrm{eq}}(r_{\mathrm{step}})}\tilde{\chi}(r_{\mathrm{step}})(\mu_1-\mu_0). \tag{A2}$$

From Eqs. (23) and (7) one obtains

$$\begin{aligned}\chi'_{\mathrm{eq}}(r_{\mathrm{step}}) &= -B_0(mJ_1(\mu_0 r_{\mathrm{step}}) + kr_{\mathrm{step}}J_0(\mu_0 r_{\mathrm{step}})),\\ g_{\mathrm{eq}}(r_{\mathrm{step}}) &= B_0(mJ_0(\mu_0 r_{\mathrm{step}}) - kr_{\mathrm{step}}J_1(\mu_0 r_{\mathrm{step}})).\end{aligned} \tag{A3}$$

Then, we can write

$$\begin{aligned}G &= r_{\mathrm{step}}\left(\frac{1}{\tilde{\chi}}\left.\frac{d\tilde{\chi}}{dr}\right|_{r=r_{\mathrm{step}^+}} - \frac{1}{\tilde{\chi}}\left.\frac{d\tilde{\chi}}{dr}\right|_{r=r_{\mathrm{step}^-}}\right) = \left(\frac{z_1}{\tilde{\chi}}\left.\frac{d\tilde{\chi}}{dz_1}\right|_{z_1=z_{\mathrm{step}^+}} - \frac{z_0}{\tilde{\chi}}\left.\frac{d\tilde{\chi}}{dz_0}\right|_{z_0=z_{\mathrm{step}^-}}\right)\\ &\approx r_{\mathrm{step}}(\mu_1-\mu_0)\frac{mJ_0(\mu_0 r_{\mathrm{step}}) - kr_{\mathrm{step}}J_1(\mu_0 r_{\mathrm{step}})}{mJ_1(\mu_0 r_{\mathrm{step}}) + kr_{\mathrm{step}}J_1(\mu_0 r_{\mathrm{step}})}.\end{aligned} \tag{A4}$$

This provides the expression for G.

In order to calculate the expression (20) for the stability parameter, it is convenient to treat separately the case $0<r_s<r_{\mathrm{step}}$ and the case $r_{\mathrm{step}}<r_s<1$. Let us consider the case $0<r_s<r_{\mathrm{step}}$ first.

The expression for the eigenfunction $\tilde{\chi}$ for arbitrary m reads

$$\tilde{\chi} = \begin{cases} kz_0[J_{m-1}(z_0)-\lambda_1 Y_{m-1}(z_0)] + m(\mu_0-k)[J_m(z_0)-\lambda_1 Y_m(z_0)] & \text{if } 0 \le z_0 \le z_s,\\ kz_0[J_{m-1}(z_0)-\lambda_2 Y_{m-1}(z_0)] + m(\mu_0-k)[J_m(z_0)-\lambda_2 Y_m(z_0)] & \text{if } z_s \le z_0 \le z_{\mathrm{step}^-},\\ kz_1[J_{m-1}(z_1)-\lambda_3 Y_{m-1}(z_1)] + m(\mu_1-k)[J_m(z_1)-\lambda_3 Y_m(z_1)] & \text{if } z_{\mathrm{step}^+} \le z_1 \le z_a, \end{cases} \tag{A5}$$

where $z_s=\sqrt{\mu_0^2-k^2}r_s$. The constraints (30) and (31) imply $\lambda_1=0$ and $\lambda_3=[kz_aJ_{m-1}(z_a)+m(\mu_1-k)J_m(z_a)]/[kz_aY_{m-1}(z_a)+m(\mu_1-k)Y_m(z_a)]$, respectively. Having determined the expression for λ_3 implies that now $(1/\tilde{\chi})(d\tilde{\chi}/dz_1)|_{z_1=z_{\text{step}^+}}$ has no arbitrary constants. Given that G is also a known quantity, one can obtain λ_2 from the boundary condition (34). This yields

$$\lambda_2=\frac{\mathcal{C}-\mathcal{E}\left(\frac{1}{\tilde{\chi}}\left.\frac{d\tilde{\chi}}{dz_1}\right|_{z_1=z_{\text{step}^+}}-G\right)}{\mathcal{D}-\mathcal{F}\left(\frac{1}{\tilde{\chi}}\left.\frac{d\tilde{\chi}}{dz_1}\right|_{z_1=z_{\text{step}^+}}-G\right)}, \tag{A6}$$

where

$$\mathcal{C}=kz_{\text{step}^-}J_{m-1}(z_{\text{step}^-})+\frac{k}{2}z_{\text{step}^-}^2[J_{m-2}(z_{\text{step}^-})-J_m(z_{\text{step}^-})]+m\frac{z_{\text{step}^-}}{2}(\mu_0-k)[J_{m-1}(z_{\text{step}^-})-J_{m+1}(z_{\text{step}^-})],$$

$$\mathcal{D}=kz_{\text{step}^-}Y_{m-1}(z_{\text{step}^-})+\frac{k}{2}z_{\text{step}^-}^2[Y_{m-2}(z_{\text{step}^-})-Y_m(z_{\text{step}^-})]+m\frac{z_{\text{step}^-}}{2}(\mu_0-k)[Y_{m-1}(z_{\text{step}^-})-Y_{m+1}(z_{\text{step}^-})],$$

$$\mathcal{E}=kz_{\text{step}^-}J_{m-1}(z_{\text{step}^-})+m(\mu_0-k)J_m(z_{\text{step}^-}),$$

$$\mathcal{F}=kz_{\text{step}^-}Y_{m-1}(z_{\text{step}^-})+m(\mu_0-k)Y_m(z_{\text{step}^-}).$$

The final expression for $r_s\Delta'$ can then be written as

$$\begin{aligned}r_s\Delta'=&z_s\frac{k[J_{m-1}(z_s)-\lambda_2Y_{m-1}(z_s)]+(k/2)z_s[J_{m-2}(z_s)-J_m(z_s)-\lambda_2(Y_{m-2}(z_s)-Y_m(z_s))]}{kz_s[J_{m-1}(z_s)-\lambda_2Y_{m-1}(z_s)]+m(\mu_0-k)(J_m(z_s)-\lambda_2Y_m(z_s))}\\&+z_s\frac{(m/2)[\mu_0-k)(J_{m-1}(z_s)-J_{m+1}(z_s)-\lambda_2(Y_{m-1}(z_s)-Y_{m+1}(z_s))]}{kz_s(J_{m-1}(z_s)-\lambda_2Y_{m-1}(z_s))+m(\mu_0-k)(J_m(z_s)-\lambda_2Y_m(z_s))}\\&-z_s\frac{kJ_{m-1}(z_s)+(k/2)z_s(J_{m-2}(z_s)-J_m(z_s))+(m/2)(\mu_0-k)(J_{m-1}(z_s)-J_{m+1}(z_s))}{kz_sJ_{m-1}(z_s)+m(\mu_0-k)J_m(z_s)},\end{aligned} \tag{A7}$$

with λ_2 given by Eq. (A6).

For $m=1$, using the recurrence relations for Bessel functions and the identity (9), Eq. (A7) can be simplified to give

$$r_s\Delta'=-\frac{2}{\pi}\lambda_2\frac{(\mu_0^2-k^2)(1+k^2r_s^2)}{G_{0J}(G_{0J}-\lambda_2G_{0Y})}, \tag{A8}$$

which coincides with the expression (36). If one considers the case $r_{\text{step}}<r_s<1$, the derivation proceeds in the same way, but now the solution for $\tilde{\chi}$ reads

$$\tilde{\chi}=\begin{cases}kz_0[J_{m-1}(z_0)-\lambda_1Y_{m-1}(z_0)]+m(\mu_0-k)[J_m(z_0)-\lambda_1Y_m(z_0)] & \text{if } 0\leqslant z_0\leqslant z_{\text{step}^-},\\ kz_0[J_{m-1}(z_0)-\lambda_2Y_{m-1}(z_0)]+m(\mu_0-k)[J_m(z_0)-\lambda_2Y_m(z_0)] & \text{if } z_{\text{step}^+}\leqslant z_1\leqslant z_s,\\ kz_1[J_{m-1}(z_1)-\lambda_3Y_{m-1}(z_1)]+m(\mu_1-k)[J_m(z_1)-\lambda_3Y_m(z_1)] & \text{if } z_s\leqslant z_1\leqslant z_a.\end{cases} \tag{A9}$$

The parameters λ_1 and λ_3 take the same values as in the previous case, but now in the expression for Δ' the quantity $(1/\tilde{\chi})(d\tilde{\chi}/dz_1)|_{z_1=z_s^-}$ depends on the constant λ_2. The latter is given by

$$\lambda_2=\frac{\mathcal{G}-\mathcal{I}\left(\frac{1}{\tilde{\chi}}\left.\frac{d\tilde{\chi}}{dz_0}\right|_{z_0=z_{\text{step}^-}}+G\right)}{\mathcal{H}-\mathcal{J}\left(\frac{1}{\tilde{\chi}}\left.\frac{d\tilde{\chi}}{dz_0}\right|_{z_0=z_{\text{step}^-}}+G\right)}, \tag{A10}$$

where

$$\mathcal{G}=kz_{\text{step}^+}J_{m-1}(z_{\text{step}^+})+\frac{k}{2}z_{\text{step}^+}^2[J_{m-2}(z_{\text{step}^+})-J_m(z_{\text{step}^+})]+m\frac{z_{\text{step}^+}}{2}(\mu_1-k)[J_{m-1}(z_{\text{step}^+})-J_{m+1}(z_{\text{step}^+})],$$

$$\mathcal{D}=kz_{\text{step}^+}Y_{m-1}(z_{\text{step}^+})+\frac{k}{2}z_{\text{step}^+}^2[Y_{m-2}(z_{\text{step}^+})-Y_m(z_{\text{step}^+})]+m\frac{z_{\text{step}^+}}{2}(\mu_1-k)[Y_{m-1}(z_{\text{step}^+})-Y_{m+1}(z_{\text{step}^+})],$$

$$\mathcal{E}=kz_{\text{step}^+}J_{m-1}(z_{\text{step}^+})+m(\mu_1-k)J_m(z_{\text{step}^+}),$$

$$\mathcal{F} = kz_{\text{step}^+}Y_{m-1}(z_{\text{step}^+}) + m(\mu_1 - k)Y_m(z_{\text{step}^+}).$$

The expression for $r_s\Delta'$ for $r_{\text{step}} < r_s < 1$ then reads

$$\begin{aligned} r_s\Delta' = {} & z_s \frac{k[J_{m-1}(z_s) - \lambda_3 Y_{m-1}(z_s)] + (k/2)z_s[J_{m-2}(z_s) - J_m(z_s) - \lambda_3(Y_{m-2}(z_s) - Y_m(z_s))]}{kz_s(J_{m-1}(z_s) - \lambda_3 Y_{m-1}(z_s)) + m(\mu_1 - k)(J_m(z_s) - \lambda_3 Y_m(z_s))} \\ & + z_s \frac{(m/2)(\mu_1 - k)[J_{m-1}(z_s) - J_{m+1}(z_s) - \lambda_3(Y_{m-1}(z_s) - Y_{m+1}(z_s))]}{kz_s(J_{m-1}(z_s) - \lambda_3 Y_{m-1}(z_s)) + m(\mu_1 - k)(J_m(z_s) - \lambda_3 Y_m(z_s))} \\ & - z_s \frac{k(J_{m-1}(z_s) - \lambda_2 Y_{m-1}(z_s)) + (k/2)z_s[J_{m-2}(z_s) - J_m(z_s) - \lambda_2(Y_{m-2}(z_s) - Y_m(z_s))]}{kz_s(J_{m-1}(z_s) - \lambda_2 Y_{m-1}(z_s)) + m(\mu_1 - k)(J_m(z_s) - \lambda_2 Y_m(z_s))} \\ & + \frac{(m/2)(\mu_1 - k)[J_{m-1}(z_s) - J_{m+1}(z_s) - \lambda_2(Y_{m-1}(z_s) - Y_{m+1}(z_s))]}{kz_s(J_{m-1}(z_s) - \lambda_2 Y_{m-1}(z_s)) + m(\mu_1 - k)(J_m(z_s) - \lambda_2 Y_m(z_s))}. \end{aligned} \tag{A11}$$

For modes $m=1$, this expression can be rewritten in the form given in Eq. (38).

APPENDIX B: IDEAL $m=1$ STABILITY

According to Newcomb's analysis,[40] if the eigenfunction $\tilde{\chi}$ corresponding to a nonresonant mode (m,k) has a zero at a radius between 0 and 1, then that mode is ideally unstable. With regard to resonant modes, crossing the threshold of ideal instability would reflect in the presence of vertical asymptotes in the graph of Δ' as a function of r_s, corresponding to the vanishing of the eigenfunction at a resonant radius. Figure 6 shows the presence of two vertical asymptotes in the case of the μ-stepped equilibrium. Such asymptotes, however, as already pointed out in Sec. III, are not due to the vanishing of $\tilde{\chi}$ and therefore do not represent a signature of ideal instability. However Fig. 7 indicates that an ideal instability could occur for a larger value of $\Delta\mu$ at a later stage of the evolution through the sequence of stepped-μ equilibria.

With regard to nonresonant modes, Newcomb's criterion can be cast into a form that turns out to be particularly convenient in our case. An indication of the presence of a zero of $\tilde{\chi}$ between 0 and 1 can be obtained with the following reasoning. If the mode were ideally marginally stable, then a smooth eigenfunction $\tilde{\chi}$ would satisfy both the boundary conditions (30) and (31) and thus would vanish at $r=0$ and at $r=1$. If we chose an arbitrary radius $\bar{r}$ such that $0<\bar{r}<1$, then the value of the quantity $(1/\tilde{\chi}(\bar{r}))(\tilde{\chi}'(\bar{r}^+)-\tilde{\chi}'(\bar{r}^-))$ would of course be zero due to the differentiability of $\tilde{\chi}$ at $\bar{r}$.

Let us consider now two eigenfunctions. One, denoted

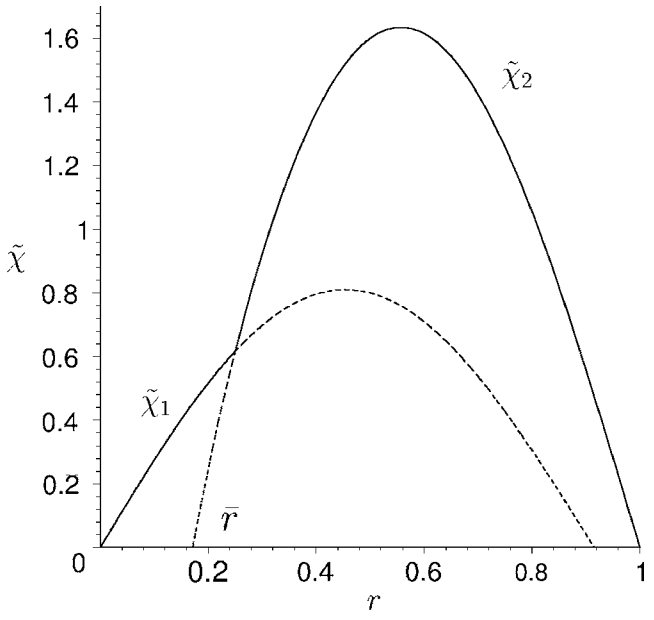

FIG. 9. The plot refers to an example of ideally unstable equilibrium. The eigenfunction $\tilde{\chi}_1$ has a zero between 0 and 1 and the eigenfunction $\tilde{\chi}_2$ satisfies the boundary condition at $r=1$. $\tilde{\chi}_1$ and $\tilde{\chi}_2$ have been plotted with a solid line for $0\leqslant r\leqslant\bar{r}$ and for $\bar{r}\leqslant r\leqslant 1$, respectively, and with a dashed line elsewhere. One can then see from the slopes of the solid lines at $r=\bar{r}=0.25$ (value of $\bar{r}$ chosen for this example) that the difference in the logarithmic derivative Δ is positive, which indicates instability. The plot refers to $(m=1,\ k=0.863)$ perturbations of a Taylor equilibrium with $\mu_T=3.5$.

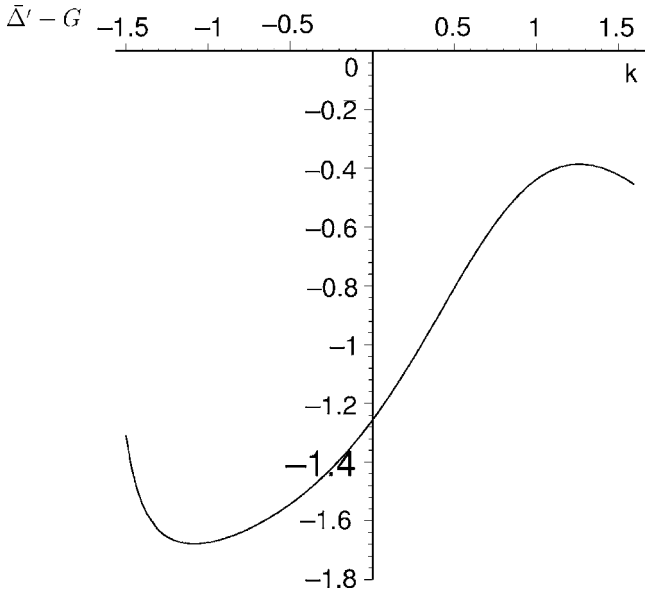

FIG. 10. Plot showing the quantity $\bar{\Delta}'-G$ for the stepped-μ equilibrium characterized by the values of the parameters given in Fig. 5. The quantity $\bar{\Delta}'-G$ is negative over the entire range of values of nonresonant wave numbers k, thus indicating ideal stability of the equilibrium.

by $\tilde{\chi}_1$, satisfying the regularity condition at $r=0$ and with a zero between 0 and 1 (to be definite let us consider the case in which this function takes a negative value at $r=1$); the other, denoted by $\tilde{\chi}_2$, satisfying the conditions $\tilde{\chi}_2(1)=0$ and $\tilde{\chi}_2(\bar{r})=\tilde{\chi}_1(\bar{r})$, but not necessarily the condition at $r=0$ (see Fig. 9). Let us assume also that $\tilde{\chi}_1'(0)$ and $\tilde{\chi}_2'(1)$ have opposite sign. The quantity $\bar{\Delta}'=[1/\tilde{\chi}_2(\bar{r})]\tilde{\chi}_2'(\bar{r}^+)-[1/\tilde{\chi}_1(\bar{r})]\tilde{\chi}_1'(\bar{r}^-)$ would then be positive. On the other hand, if $\tilde{\chi}_1$ has no zeroes between 0 and 1, $\bar{\Delta}'$ would be negative. This implies that the sign of the quantity $\bar{\Delta}'$ determines whether an eigenfunction has a zero or not and consequently it allows to reach a conclusion on the ideal stability of the equilibrium with respect to that perturbation. In our case, the eigenfunctions have a discontinuous derivative at r_{step} and the condition for determining the presence of a zero in $\tilde{\chi}_1$ can be conveniently found choosing $\bar{r}=r_{\text{step}}$. The criterion then reduces to checking whether the quantity $\bar{\Delta}'$ is greater or less than the jump in the logarithmic derivative G. In the first case, the equilibrium is unstable, whereas $\bar{\Delta}'<G$ means stability.

The plot in Fig. 10 shows the difference $\bar{\Delta}'-G$ for values of the parameters corresponding to the example considered in Sec. III. It is clear from the plot that in the considered range of k, which corresponds to nonresonant surfaces, $\bar{\Delta}'-G$ is always negative, thus implying ideal stability of the equilibrium.

[1] See, e.g., S. Ortolani and D. D. Schnack, *Magnetohydrodynamics of Plasma Relaxation* (World Scientific, Singapore, 1993), and references cited therein.
[2] See, e.g., H. A. B. Bodin, and A. A. Newton, Nucl. Fusion **20**, 1255 (1980), and references cited therein.
[3] J. B. Taylor, Phys. Rev. Lett. **33**, 1139 (1974); Rev. Mod. Phys. **58**, 741 (1986).
[4] R. D. Gibson and K. J. Whiteman, Plasma Phys. **10**, 1101 (1968).
[5] B. Coppi, J. M. Greene, and J. L. Johnson, Nucl. Fusion **6**, 101 (1966).
[6] H. P. Furth, J. Killeen, and M. N. Rosenbluth, Phys. Fluids **6**, 459 (1963).
[7] D. C. Robinson, Plasma Phys. **13**, 439 (1971).
[8] D. C. Robinson, Nucl. Fusion **18**, 939 (1978).
[9] V. Antoni, D. Merlin, S. Ortolani, and R. Paccagnella, Nucl. Fusion **26**, 1711 (1986).
[10] P. Martin, L. Marrelli, G. Spizzo, P. Franz, P. Piovesan, I. Predebon, T. Bolzonella, S. Cappello, A. Cravotta, D. F. Escande, L. Frassinetti, S. Ortolani, R. Paccagnella, D. Terranova, the RFX Team, B. E. Chapman, D. Craig, S. C. Prager, J. S. Sarff, the MST Team, P. Brunsell, J.-A. Malmberg, J. Drake, the EXTRAP T2R Team, Y. Yagi, H. Koguchi, Y. Hirano, the TPE-RX Team, R. B. White, C. Sovinec, C. Xiao, R. A. Nebel, and D. D. Schnack, Nucl. Fusion **43**, 1855 (2003).
[11] P. R. Brunsell, Y. Yagi, Y. Hirano, Y. Maejima, and T. Shimada, Phys. Fluids A **5**, 885 (1993).
[12] P. Nordlund and S. Mazur, Phys. Plasmas **1**, 4032 (1994).
[13] J. S. Sarff, N. E. Lanier, S. C. Prager, and M. R. Stoneking, Phys. Rev. Lett. **78**, 62 (1997).
[14] D. F. Escande, P. Martin, S. Ortolani, A. Buffa, P. Franz, L. Marrelli, E. Martines, G. Spizzo, S. Cappello, A. Murari, R. Pasqualotto, and P. Zanca, Phys. Rev. Lett. **85**, 1662 (2000); D. F. Escande, S. Cappello, F. D'Angelo, P. Martin, S. Ortolani, and R. Paccagnella, Plasma Phys. Controlled Fusion **42**, B243 (2000).
[15] Y. Hirano, R. Paccagnella, H. Koguchi, L. Frassinetti, H. Sakakita, S. Kiyama, and Y. Yagi, Phys. Plasmas **12**, 112501 (2005).
[16] L. Frassinetti, I. Predebon, H. Koguchi, Y. Yagi, Y. Hirano, H. Sakakita, G. Spizzo, and R. B. White, Phys. Rev. Lett. **97**, 175001 (2006).
[17] S. Cappello and R. Paccagnella, in *Proceeding of the Workshop on Theory of Fusion Plasmas*, edited by E. Sindoni (Compositori, Bologna, 1990), p. 595; Phys. Fluids B **4**, 1662 (1992).
[18] J. M. Finn, R. A. Nebel, and C. C. Bathke, Phys. Fluids B **4**, 1262 (1992).
[19] S. Cappello and R. Paccagnella, Nucl. Fusion **36**, 571 (1996).
[20] S. Ortolani and the RFX team, Plasma Phys. Controlled Fusion **48**, B371 (2006).
[21] S. von Goeler, W. Stodiek, and N. Sauthoff, Phys. Rev. Lett. **33**, 1201 (1974).
[22] M. Kotschenreuther, R. D. Hazeltine, and P. J. Morrison, Phys. Fluids **28**, 294 (1985).
[23] J. D. Callen, W. X. Qu, D. Siebert, B. A. Carreras, K. C. Shaing, and D. A. Spong, in *Plasma Physics and Controlled Nuclear Fusion Research* (IAEA, Vienna, 1987), Vol. 2, p. 157.
[24] R. Carrera, R. D. Hazeltine, and M. Kotschenreuther, Phys. Fluids **29**, 899 (1986).
[25] T. G. Cowling, Mon. Not. R. Astron. Soc. **94**, 39 (1933).
[26] G. Rostagni, Fusion Eng. Des. **25**, 301 (1995).
[27] N. Arcis, D. F. Escande, and M. Ottaviani, Phys. Plasmas **14**, 032308 (2007).
[28] D. Voslamber and D. K. Callebaut, Phys. Rev. **128**, 2016 (1962).
[29] R. Paccagnella (private communication, 2007).
[30] E. Joffrin, C. D. Challis, G. D. Conway, X. Garbet, A. Gude, S. Guenter, N. C. Hawkes, T. C. Hender, D. F. Howell, G. T. A. Huysmans, E. Lazzaro, P. Maget, M. Marachek, A. G. Peeters, S. D. Pinches, S. E. Sharapov, and JET-EFDA Contributors, Nucl. Fusion **43**, 1167 (2003).
[31] M. Hole, S. R. Hudson, and R. L. Dewar, J. Plasma Phys. **72**, 1167 (2006).
[32] S. R. Hudson, M. Hole, and R. L. Dewar, Phys. Plasmas **14**, 052505 (2007).
[33] M. Hole, S. R. Hudson, and R. L. Dewar, Nucl. Fusion **47**, 746 (2007).
[34] F. Militello and F. Porcelli, Phys. Plasmas **11**, L13 (2004).
[35] D. F. Escande and M. Ottaviani, Phys. Lett. A **323**, 278 (2004).
[36] R. J. Hastie, F. Militello, and F. Porcelli, Phys. Rev. Lett. **95**, 065001 (2005).
[37] N. Arcis, D. F. Escande, and M. Ottaviani, Phys. Lett. A **347**, 241 (2005).
[38] N. Arcis, D. F. Escande, and M. Ottaviani, Phys. Plasmas **13**, 052305 (2006).
[39] F. Militello, R. J. Hastie, and F. Porcelli, Phys. Plasmas **13**, 112512 (2006).
[40] W. A. Newcomb, Ann. Phys. (Paris) **10**, 232 (1960).